

ELECTRON PARAMAGNETIC RESONANCE OF AN Fe–Fe PAIR IN SILICON

J.J. van Kooten, E.G. Sieverts and C.A.J. Ammerlaan

Natuurkundig Laboratorium der Universiteit van Amsterdam, Valckenierstraat 65, 1018 XE Amsterdam,
The Netherlands

(Received 9 July 1987 by B. Mühlischlegel)

The electron paramagnetic resonance spectrum Si-NL24, which is associated with an iron–iron impurity pair and was earlier observed in electron-irradiated silicon, was produced as a quenched-in defect spectrum. Contrary to previous work we could resolve the complete angular dependence of the spectrum and found that it has monoclinic I symmetry. Two possible atomic models with the iron atoms at interstitial sites are presented. The EPR spectrum can be described as a paramagnetic system with $S = 1/2$ and rather unusual g -values, as well as by $S = 5/2$ and g -values close to $g = 2$. Hyperfine interactions with two equivalent ^{57}Fe nuclei could be determined. This Fe–Fe pair and the Fe_4 complex are the only intermediate states in the thermal clustering process of interstitial iron which are observed in electron paramagnetic resonance.

1. INTRODUCTION

IRON IS ALMOST INEVITABLY present as an unwanted impurity in silicon crystals. Because of its high diffusion coefficient, isolated interstitial iron is unstable even at room temperature and tends to form complexes with other impurities. Most iron-related centres are electrically active and therefore deteriorate device properties. Deep level transient spectroscopy (DLTS) measurements revealed the donor level Fe^{+0} of single interstitial iron and of the impurity pairs formed between iron and the shallow acceptors [1–6]. In photoluminescence (PL) the spectra of FeB and FeIn were reported [7–10], although the identifications are not unambiguous due to the lack of an observable iron isotope shift. Electron paramagnetic resonance (EPR) of iron and iron-acceptor pairs was reported in the early sixties by Ludwig and Woodbury [11] and, more recently, by others [12–14]. More complicated iron-related EPR spectra were reported by Muller *et al.* [15]. They studied the clustering of iron in iron-diffused, electron-irradiated silicon. The disappearance of iron-related EPR, DLTS, and PL spectra after annealing or even after prolonged storage at room temperature is due to the formation of bigger complexes which can for instance be demonstrated by the phenomenon of haze after etching of polished silicon surfaces [16, 17].

A first step towards the formation of larger clusters, are defects containing two to four iron atoms. In this respect the EPR spectra Si-NL20 to NL25 [15, 18]

are important. These spectra were detected in electron-irradiated material, but the proposed atomic models for spectra NL22 and NL24 [15] do not contain vacancies or self-interstitials, and can be expected to be present in non-irradiated material as well. For NL22, identified as a four-iron complex, this was observed indeed. The original observation of NL24 was obscured by other spectra. Consequently no complete angular dependence could be measured. The angular variation of the spectrum resembled a pattern characteristic for rhombic II symmetry. Because of the fact that in such a symmetry six orientations exist, with only three different resonances when measuring in a $\{0\ 1\ 1\}$ plane, while ten different lines were observed, it was concluded that the symmetry must be lower. It was speculated to be monoclinic II, point-group 2 ($2_{\langle 100 \rangle}$). In this Communication we report the observation of an EPR spectrum, directly after quenching the iron diffused sample, which strongly resembles NL24. We could resolve the complete angular dependence of the spectrum and therefore determine the correct symmetry.

Experimental details of sample preparation and the K-band spectrometer are similar as described in [13]. Besides this NL24 EPR spectrum also spectra of Fe_i^0 , Fe_i^+ , NL27 (FeAl_I) and NL28 (FeAl_{II}), were observed.

2. RESULTS

Directly after the quench, following the iron dif-

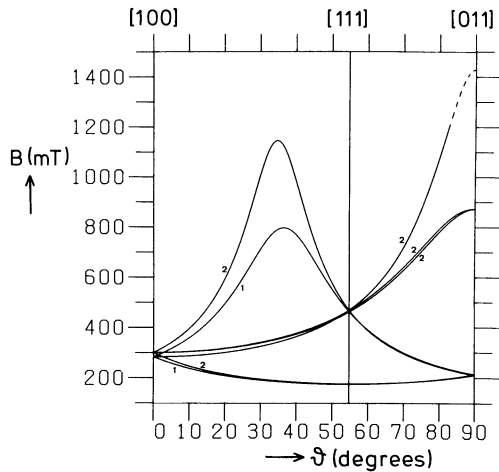


Fig. 1. Angular dependence of the observed monoclinic I EPR spectrum, simulated with microwave frequency $\nu = 23$ GHz, magnetic field \mathbf{B} in the $(0\bar{1}1)$ plane, and with parameters as given in the first column of Table I. Figures along the curves indicate orientational degeneracies. In the region above $B = 1200$ mT, shown dashed, no experimental observations could be made.

fusion at $T = 1200^\circ\text{C}$, we observed an EPR spectrum whose angular dependence is plotted in Fig. 1. Due to instrumental limitations, the part of the spectrum at magnetic field values exceeding 1.2 T was not actually observed. The symmetry of the depicted pattern is monoclinic I, i.e. pointgroup $2(2_{\langle 011 \rangle})$, m , or $2/m$. The resonances disappeared already after room temperature storage of half a day. The spectrum could be fitted with an effective spin $S = 1/2$ and a spin Hamiltonian which only contains the electronic Zeeman interaction:

$$H = \mu_B \mathbf{B} \cdot \mathbf{g} \cdot \mathbf{S}. \quad (1)$$

The resulting principal values and directions of the g -tensor are listed in Table 1. The mean deviation between the calculated transitions of this fit and the measured data was 0.4 mT. However, it appeared that there was a systematic deviation up to 10 mT between the fit and data near the maximum at $\theta \sim 35^\circ$, $B \sim 1150$ mT (Fig. 1). Somewhat better results could be obtained with an effective spin $S = 5/2$ and an additional zero-field splitting term in the spin Hamil-

Table 1. Spin Hamiltonian parameters of the observed EPR spectrum, identified with Si-NL24. Given are principal values of g , of the zero-field splitting term D , and of the ^{57}Fe hyperfine interaction A . Angles θ are between the directions of the first principal values and $[0\bar{1}1]$. The second principal value is always parallel to $[0\bar{1}1]$. Also reduced values of D and A are given (see text). Values of D and A are in MHz. Given values result from least squares fits under various constraints or start values

| S | 1/2 | 5/2 | 5/2 | 5/2 | 5/2 |
|-------------|--------------|--------------|----------------------|-----------------------|--------------|
| g_1 | 9.44 | 2.303 | 2.259 | 1.583 | 2.07 |
| g_2 | 1.15 | 2.046 | 1.957 | 1.449 | 2.07 |
| g_3 | 2.06 | 1.870 | 1.803 | 2.202 | 2.07 |
| θ_g | 36.4° | 78.6° | 69.2° | 36.4° | — |
| D_1 | — | —53.9 | —48.4 | —34.7 | —47.4 |
| D_2 | — | 67.2 | 61.4 | 48.7 | 59.2 |
| D_3 | — | —13.3 | —13.0 | —14.0 | —11.8 |
| θ_D | — | 29.8° | 29.7° | 36.4° | 36.4° |
| A_1 | — | 9.2 | 9.3 | 9.8 | 8.8 |
| A_2 | — | 17.7 | 18.5 | 13.7 | 19.6 |
| A_3 | — | 6.3 | 6.0 | 5.2 | 9.9 |
| θ_A | — | 29.5° | 36.9° | 27.9° | 74.8° |
| constraints | — | — | — | $\theta_g = \theta_D$ | $g = 2.07$ |
| start | — | $g = 2$ | $E/D = -\frac{1}{2}$ | — | — |
| \bar{g} | (4.22) | 2.073 | 2.006 | 1.745 | 2.07 |
| D | — | —80.9 | —72.6 | —52.1 | —71.1 |
| E | — | 40.3 | 37.2 | 31.4 | 35.5 |
| E/D | — | —0.498 | —0.512 | —0.603 | —0.499 |
| a | — | 11.1 | 11.2 | 9.6 | 12.8 |
| b | — | 3.3 | 3.8 | 2.1 | 3.4 |

tonian

$$H = \mu_B \mathbf{B} \cdot \mathbf{g} \cdot \mathbf{S} + \mathbf{S} \cdot \mathbf{D} \cdot \mathbf{S}. \quad (2)$$

In this case, however, the system was found to be underdetermined. This means that in practice no unique set of parameters can be determined and that in a least squares computer fit no absolute minimum can be found. This is reminiscent of a similar situation for spectrum NL21 [18].

In order to obtain physically relevant results some suppositions on the electronic g -values and the zero-field splitting must be made. In an analytic solution, an equivalence between the $S = 1/2$ description and a description with $S = 5/2$ and g -values close to $g = 2$ can be shown [19]. Using the results of this treatment as start parameters, satisfactory fits could be made, which are also shown in Table 1. The electronic g -values are close to $g = 2$ indeed, and the maximum deviations between the fits and the data were in these cases 4 mT at most. Results clearly depend on chosen constraints and start parameters. In this low symmetry the zero-field splitting is often described by an axial crystal field term D and a rhombic term E . These terms are related to the principal values of the tensor \mathbf{D} by $D_1 = \frac{2}{3}D$, $D_2 = -\frac{1}{3}D + E$, $D_3 = -\frac{1}{3}D - E$. Addition to the spin Hamiltonian of allowed higher order terms in the spin only marginally improved the computer fits. Therefore no data on these terms are included in Table 1. Although the description with $S = 1/2$ gives a poorer fit and no physically meaningful parameters, it has yet the great advantage that it allows a unique description of the system.

Results of an analysis of ^{57}Fe hyperfine interactions are also included in Table 1. They could be obtained from older measurements by Muller [20] on a sample isotopically enriched to 85% in ^{57}Fe . Besides principal values of the hyperfine tensor, also resulting values for the isotropic part a and the anisotropic axial part b are given. In the $S = 1/2$ description no satisfactory fit for the hyperfine interaction could be obtained.

3. DISCUSSION

An EPR spectrum in silicon with the present symmetry and g -values has not been reported in the literature. However, we can show that the paramagnetic centre observed here is the same as centre NL24, described by Muller [15, 18]. Centre NL24 was observed after electron irradiation of iron-diffused silicon. The spectrum disappeared when annealing the sample at 75°C for only one hour. The analysis of the spectrum was hampered because the spectrum was obscured by other resonances due to many different paramagnetic centres present after electron irradiation.

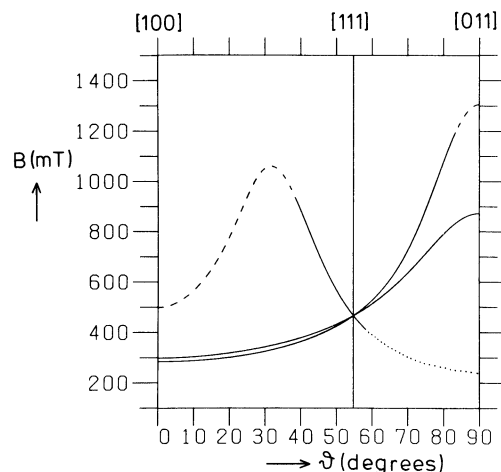


Fig. 2. Simulation ($\nu = 23$ GHz, \mathbf{B} in the $(0\bar{1}1)$ plane) of EPR spectrum Si-NL24 as reported by Muller *et al.* [15]. Along the dashed line no resonances had been observed. Resonances along the dotted line had not been used to fit the spectrum.

Inspection of Fig. 10 of Muller *et al.* [15] and our Fig. 1 reveals a striking similarity between NL24 and three branches of the angular pattern of the present spectrum. For a better comparison, we simulated the EPR transitions of NL24 by computer diagonalisation of the Hamiltonian used by Muller [15]. The simulated angular dependence of the original spectrum NL24 is depicted in Fig. 2. It is noted that average positions of groups of lines have been used to obtain this fit. Only along the full lines resonances were observed that were used in the fit [15, 18, 20]. If we keep in mind that Fig. 2 represents average positions of resonance lines, we observe that branches in Fig. 2 coincide with branches in Fig. 1. Furthermore, the measurements of NL24 which had not been used for the fit, along the dotted part in Fig. 2, are much better represented by the monoclinic I Hamiltonian (Fig. 1) than by the rhombic II Hamiltonian (Fig. 2). Moreover, the wide splitting of the high field lines, when rotating the magnetic field from $[1\bar{1}1]$ to 40° , completely reproduced data in these old measurements [20]. Although Muller described the spectrum with a rhombic II Hamiltonian (pointgroup 222), she concluded that the actual symmetry must be lower ("probably 2"). The reason was that 222 symmetry gives only three resonances or with a tilted sample at most six, while ten different lines were observed, "grouped with two or four lines together". A monoclinic I centre has 12 different orientations in the silicon lattice, that are related by the symmetry operations of the lattice. When measuring in a $\{0\bar{1}1\}$ plane only seven resonances will be observed because of the additional symmetry. This means that all but two

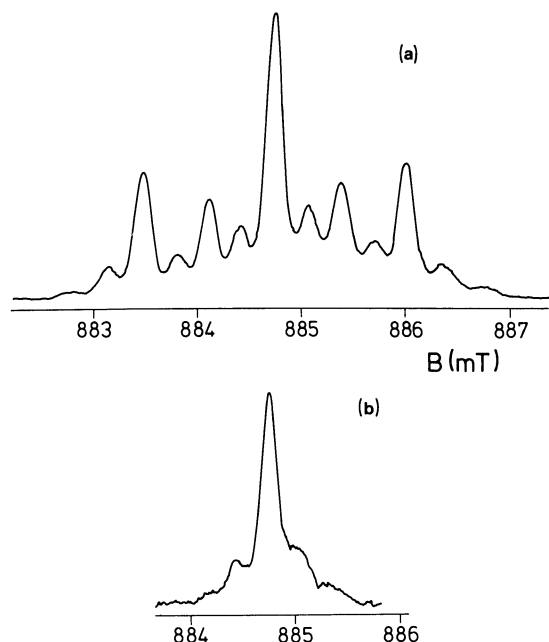


Fig. 3. Lineshape of EPR spectrum Si-NL24; (a) in a sample doped with iron enriched to 85% in the isotope ^{57}Fe ; and (b) in a sample doped with natural iron. (After Muller [18]). The magnetic field is in the $(0\bar{1}1)$ plane, at 75° from $[100]$. The sample temperature was 1.4 K.

branches in Fig. 1 are two-fold degenerate. These degeneracies are indicated. In case of a slight misorientation of the sample all 12 lines in such a highly anisotropic spectrum can be separately observed. Figure 2 shows that Muller did not observe the two lowest branches in Fig. 1, that is in case of misalignment three lines. In Muller's original measurements around the $[111]$ direction in the 450 mT region indeed a total of nine lines is found [20]. The tenth line which she noticed is probably observed close to $[011]$ where three of the lines at $[111]$ come down to about 210 mT and join the low-field branches which she did not observe at other angles. Moreover, in that region lines due to spectrum NL21 were present in her case. All these facts and the striking conformity between these rare, very anisotropic spectra are convincing arguments that our spectrum is identical to NL24. Also the annealing characteristics are in agreement.

Figure 3(a) shows the lineshape of spectrum NL24 in a sample doped with iron enriched to 85% with ^{57}Fe (nuclear spin $I = 1/2$) as reported in [18]. The five strongest lines in this figure represent the hyperfine structure due to iron. From the splitting and intensity ratios of the Fe hyperfine lines, it is concluded that the centre consists of two equivalent iron atoms [18]. The calculated intensity ratios 18:13:38:13:18 on the basis of 85% enrichment are exactly reproduced in the experimental spectrum. A

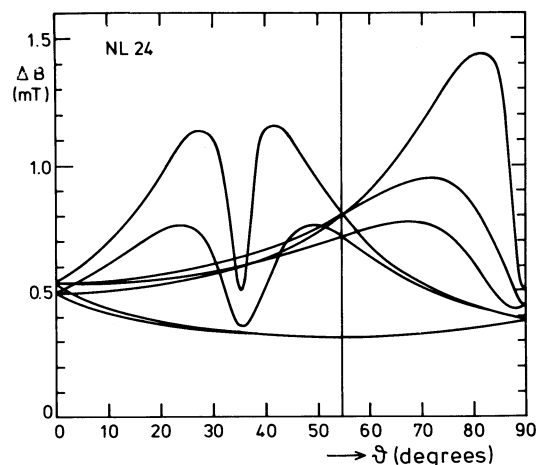


Fig. 4. Angular dependence of the ^{57}Fe hyperfine splitting ΔB of spectrum Si-NL24, as calculated from the fitted parameters in the last column of Table 1 ($\nu = 23$ GHz, \mathbf{B} in the $(0\bar{1}1)$ plane).

plot of the fitted angular dependence of the Fe hyperfine splitting is shown in Fig. 4. In between the Fe hyperfine lines in Fig. 3(a) lines due to hyperfine interaction with ^{29}Si are visible. This interaction is more easily recognised in Fig. 3(b) where no iron splitting is present. From the intensity of the lines for this particular direction of the magnetic field in which several hyperfine lines accidentally coincide, it follows that interaction with at least eight silicon neighbours is observed [18].

In the model proposed in [15, 18], the iron atoms are situated at interstitial T positions. Our observation of NL24 directly after quenching of the sample, further corroborates the assumption that the iron atoms occupy their normal interstitial positions. However, a configuration of different symmetry is required. A possible model for a two-iron centre with intrinsic $2/m$ symmetry is shown in Fig. 5(a). As an alternative a simpler model of two iron atoms at nearest T interstitial sites is given in Fig. 5(b). The model as shown has only trigonal symmetry. If we decompose the principal g -values in the $S = 1/2$ description as

$$\begin{aligned} g_1 &= g + 2f, & g_2 &= g - f - h, \\ g_3 &= g - f + h, \end{aligned} \quad (3)$$

where g is the isotropic part or average value, f is the axial component, and h the deviation from axial symmetry, we find $g = 4.22$, $f = 2.61$, $h = 0.46$. The relative deviation from axiality, measured by h/f , is only 0.18 which is an indication that the centre is predominantly axially symmetric, with the axial direction g_1 closely parallel to $[111]$. This indicates that only a rather small distortion from the trigonal structure in Fig. 5(b) is required to account for the obser-

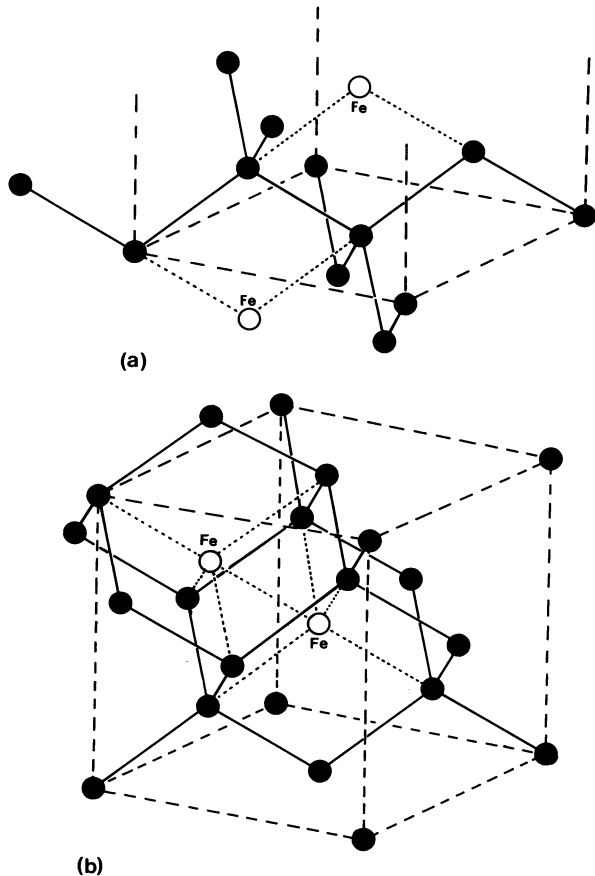


Fig. 5. Possible atomic models of the Fe-Fe pair in silicon, corresponding to EPR spectrum NL24; (a) configuration with intrinsic $2/m$ symmetry; (b) configuration of two nearest T interstitial sites with trigonal symmetry, i.e. before distortion.

ved lower monoclinic I symmetry. It should be noted that in the analysis with $S = 5/2$ the anisotropy of the centre is primarily represented by the D -tensor. The axial direction of this tensor is also close to $[111]$.

As for the charge state of the centre, we note the following. Muller observed NL24 in high resistivity n - and p -type material and concluded that the centre could be either in the neutral or in the singly positive charge state. We detected the spectrum in $1\Omega\text{cm}$ p -type material, but since both Fe_i^0 and Fe_i^+ were present in the same sample this does not exclude either charge state. The spectrum can only be fitted with half-integer spin. This fact rules out the possibility of two neutral iron atoms. Isolated Fe_i^0 has a spin $S = 1$ and in case of a neutral pair the spins are coupled to a resulting integer spin. From the simultaneous observation with Fe_i^+ a singly positive charge state of the defect is more probable than a negative one.

In the nearest neighbour $(\text{Fe}_i - \text{Fe}_i)^+$ model the d orbitals on the two iron atoms can experience an

appreciable mutual interaction because of their small distance. This interaction may very well be larger than repulsive Coulombic interactions, which can lead to an ordering of molecular orbital states which is no longer in accord with Hund's rule and results in a low-spin state with $S = 1/2$ [21]. However, the unusual g -values of up to $g = 9.44$ cannot be explained in that case. Moreover, the ^{57}Fe hyperfine interactions are found to be axial along $[0\bar{1}1]$, i.e. perpendicular to the mirrorplane of the defect, instead of along the connection line between the iron atoms. As g -values close to 2 can only result from a spin Hamiltonian with $S = 5/2$, we prefer a description in which 5 missing d -electrons are coupled with their spins parallel. This naturally results in a singly positive charge state of the defect. In view of the experimental observation that both iron atoms are equivalent, the electron which misses with respect to the neutral state will be shared by the two iron atoms.

The value of the isotropic part of the iron hyperfine interaction of NL24 is very close to the values found for similar two-iron, $S = 5/2$ spectra, as NL20 and NL21 [15]. These spectra are ascribed to $\text{Fe}_i - \text{Fe}_i - \text{V}$ and $\text{Fe}_i - \text{Fe}_i - \text{V}_2$ complexes, respectively, in which V indicates a lattice vacancy. When taking into account its spin $S = 3/2$, also the Fe_iB_i pair gives a similar value [11]. In general, for transition metal impurities the isotropic part of the hyperfine interaction is ascribed to exchange polarisation of core and valence s electrons. We are thus led to the conclusion that the iron s electrons in these various centres experience very similar interactions from the polarising $3d$ electrons. The observed strong anisotropy of the hyperfine line splitting, as illustrated in Fig. 4, is found to be largely determined by other terms in the spin Hamiltonian. A fit with an isotropic hyperfine interaction $a = 9.2\text{MHz}$ is only slightly worse than with the anisotropic interactions as given in Table I. As a result, the uncertainty in the values is unexpectedly large, when compared to the accuracy with which line splittings are determined. Yet, the resulting anisotropy $b = 3.0 \pm 1.0\text{MHz}$ for the interaction with each of the two iron nuclei is quite large when compared with the value for a free ion $3d$ orbital which should be about 21MHz for a single electron at a single iron nucleus. Again for the earlier mentioned centres, similar values have been determined. When making a group theoretical analysis of allowed d orbitals in the present monoclinic symmetry, we can conclude from the observed $[0\bar{1}1]$ axiality of the hyperfine interaction that it arises primarily from electrons in either a d_{xy+zx} orbital or in a d_{xy-zx} and a d_{2-y^2} orbital. The observation of rather intense ^{29}Si hyperfine interactions which are well-resolved

from the central EPR lines for several directions of the magnetic field indicates that, besides the main localisation on the two iron ions, there is also an important transfer of unpaired electrons to at least eight surrounding silicon atoms. As these interactions could not further be analysed from EPR data, no direct relation with one of the structural models in Fig. 5 can be made. In both models, however, there are eight silicon atoms which are at nearest neighbour distance from an iron ion.

With the determination of this rather ephemeral $\text{Fe}_i\text{-Fe}_i$ centre, the first product in the important aggregation process of interstitial iron in silicon at temperatures around room temperature has unambiguously been identified. Its disappearance at or just above room temperature indicates that there is strong preference for further iron aggregation at this centre. The only other, somewhat less evanescent, intermediate state which had so far been observed in EPR is the $(\text{Fe}_i)_4$ cluster, ascribed to spectrum Si-NL22 [15, 18].

Acknowledgements — We like to thank Dr. Sara H. Muller for stimulating discussions and for making old measurement data available to us. This work received financial support from the Foundation for Fundamental Research on Matter (FOM).

REFERENCES

1. K. Wünstel, K.-H. Froehner & P. Wagner, *Physica* **116B**, 301 (1983).
2. L.C. Kimerling & J.L. Benton, *Physica* **116B**, 297 (1983).
3. L.C. Kimerling, J.L. Benton & J.J. Rubin, in: *Defects and Radiation Effects in Semiconductors 1980*, p. 217 (Edited by R.R. Hasiguti), The Institute of Physics, London, (1981).
4. A. Chantre & D. Bois, *Phys. Rev.* **B31**, 7979 (1985).
5. H. Feichtinger, *Acta Physica Austriaca* **51**, 161 (1979).
6. K. Graff & H. Pieper, *J. Electrochem. Soc.* **128**, 669 (1981).
7. G.S. Mitchard, S.A. Lyon, K.R. Elliott & T.C. McGill, *Solid State Commun.* **29**, 425 (1979).
8. M.L.W. Thewalt, U.O. Ziemelis & R.R. Parsons, *Solid State Commun.* **39**, 27 (1981).
9. J. Weber, R. Sauer & P. Wagner, *J. Lumin.* **24**, 25, 155 (1981).
10. H.D. Mohring, J. Weber & R. Sauer, *Phys. Rev.* **B30**, 894 (1984).
11. G.W. Ludwig and H.H. Woodbury, in: *Solid State Physics*, Vol. 13, p. 223 (Edited by F. Seitz and D. Turnbull), Academic, New York, (1962).
12. W. Gehlhoff and K.H. Segsa, *Phys. Status Solidi (b)* **115**, 443 (1983).
13. J.J. van Kooten, G.A. Weller & C.A.J. Ammerlaan, *Phys. Rev.* **B30**, 4564 (1984).
14. C.A.J. Ammerlaan & J.J. van Kooten, *Materials Research Society Symposium Proceedings* **46**, 525 (1985).
15. S.H. Muller, G.M. Tuynman, E.G. Sieverts & C.A.J. Ammerlaan, *Phys. Rev.* **B25**, 25 (1982).
16. W.T. Stacy, D.F. Allison & T.C. Wu, in: *Semiconductor Silicon 1981*, p. 344. (Edited by H.R. Huff *et al.*), Proceedings volume 81-5, The Electrochemical Society, Pennington, NJ, (1981).
17. K. Graff, in: *Aggregation phenomena of point defects in silicon*, p. 121 (Edited by E. Sirtl *et al.*), Proceedings volume 83-4, The Electrochemical Society, Pennington, NJ (1983).
18. S.H. Muller, Ph.D. Thesis, University of Amsterdam (1981).
19. C.A.J. Ammerlaan, to be published.
20. S.H. Muller, Private communication.
21. J.J. van Kooten, Ph.D. Thesis, University of Amsterdam, (1987).